*DOI:*
10.1021/acsphotonics.8b01083

*Document Version*
Peer reviewed version

# Förster Resonance Energy Transfer inside Hyperbolic Metamaterials

Diane J. Roth[1,*], Mazhar E. Nasir[1], Pavel Ginzburg[2], Pan Wang[1], Alix Le Marois[1], Klaus Suhling[1], David Richards[1] and Anatoly V. Zayats[1]

[1] Department of Physics, King's College London, Strand, London WC2R 2LS, United Kingdom
[2] School of Electrical Engineering, Tel Aviv University, Tel Aviv 69978, Israel

***Abstract***

The ability to control Förster Resonance Energy Transfer (FRET) between emitters via the design of nanostructured materials with appropriate electromagnetic properties is important in the development of fast and enhanced sources of illumination, high-efficiency photovoltaic devices and biomedical applications, such as nanorulers. While the engineering of the local density of states allows an efficient control over the spontaneous emission rate, its influence on the FRET process has been an ongoing debate and has led to disparate experimental and theoretical results. In particular, hyperbolic metamaterials have recently been shown to drastically increase the fluorescence decay rate. Here, we experimentally demonstrate an increase in the FRET rate for Donor-Acceptor (D-A) pairs separated by fixed distances (3.4, 6.8 and 10.2 nm) located inside a hyperbolic metamaterial comprised of an array of gold nanorods. While the modification of the local density of states surrounding the D-A pairs strongly influences the FRET rate, leading to a 13-fold increase inside the metamaterial, the FRET efficiency is shown to remain mostly unaffected. For comparison, we also study the modification of energy transfer rate and efficiencies of D-A pairs placed on top of a gold film, on top of a nanorod-based metamaterial and inside a nanorod-based metamaterial coated with polymer in order to prevent quenching. The free-space emission intensities of the acceptor were also investigated, leading up to an 18-fold increase in the emission intensity. The designed

geometry shows great potential in the development of FRET-based applications such as biomedical imaging, organic solar-cells and light-emitting sources.

KEYWORDS: Hyperbolic metamaterials, plasmonics, Förster resonance energy transfer

Förster resonance energy transfer (FRET) is the non-radiative transfer of excited state energy from a donor fluorophore to an acceptor fluorophore via a dipole-dipole coupling process. It was first correctly described by German physical chemist Theodor Förster in the 1940s (1-2), and today is a powerful tool used in various domains ranging from biophysics, in order to detect molecular interactions at the nanoscale (3-5); to organic photovoltaics (6) and light-emitting devices (7-8). While the design of nanostructured materials with appropriate electromagnetic properties has widely been shown to allow the control of spontaneous emission via the engineering of their local density of electromagnetic states (LDOS), the possibility of using these same environments to control the energy transfer between emitters has gained a lot of interest. In particular, structures such as plasmonic films (9), microcavities (10), nanoparticles (11) and nanoantennas (12-13) have been the focus of many experimental and theoretical studies, leading to contradictory results.

While an enhancement of FRET in modified electromagnetic environments has been suggested in several experimental studies (10, 14, 15) and sometimes linked to the modification of the LDOS through linear or quadratic dependences, recent theoretical findings have shown FRET and LDOS to be unrelated (16). Additionally, inhibition of FRET has also been experimentally shown (17), whereas other studies have demonstrated no influence of the electromagnetic environment on the FRET process (9,18). This lack of effect of the electromagnetic environment on FRET has however been recently related to the particular experimental parameters considered in each experimental study (16). This emphasizes the

importance of the precise control of the electromagnetic properties of the complex environments and their relation with the spectral properties of the D-A pairs, the distance and orientation of the donors and acceptors with regard to their surrounding environment but also the donor-acceptor distance within a pair. These factors have all been shown to influence the FRET process, exhibiting regimes where FRET rates and efficiencies are either enhanced or suppressed.

Recently, hyperbolic metamaterials, constituting a well-known flexible platform for the control of spontaneous emission (19-21), have also been considered for the control of the FRET process. Hyperbolic metamaterials (HMM) are strongly anisotropic materials, with a dielectric permittivity tensor having the real part of the diagonal components of opposite signs. Their unique topology provides a high density of electromagnetic states and broadband enhancement of spontaneous emission (20). Typical designs of hyperbolic metamaterials include metallo-dielectric multilayers (22), nanorod assemblies (23) or natural hyperbolic materials (24). To date, the study of FRET using hyperbolic metamaterials has been performed on a multi-layered system, for which inhibition of FRET for donor-acceptor (D-A) pairs located on top of the metamaterial was experimentally demonstrated (25); it was shown that the energy transfer rate at various distances above the metamaterial is not correlated to the Purcell factor, and therefore the LDOS, with the effect of the material environment on the energy transfer being much weaker than on the Purcell factor.

Here, we experimentally investigate the energy transfer in D-A pairs placed at the end of double stranded DNA linkers of three different lengths (10, 20 and 30 base pairs, corresponding to 3.4, 6.8 and 10.2 nm) located inside a nanorod-based hyperbolic metamaterial. The relatively straightforward and cost-effective manufacturing process of these metamaterials, using a self-assembly approach, combined with the possibility to precisely tune their geometrical parameters, allows their electromagnetic properties to be tailored in a wide

spectral range and over large areas. This study of FRET, through D-A pairs attached to rigid DNA linkers and time-resolved analysis of the emission dynamics of the donor, reveals a strongly position-dependent modification of the energy transfer characteristics, with a large increase of the FRET rate especially inside the metamaterial. The FRET efficiencies and free-space emission intensity of the acceptor have also been investigated.

## Results and Discussions

***Material environments.*** In this experimental study, five different environments were considered in order to investigate the dependence of the LDOS on the energy transfer between the donor and the acceptor. A glass coverslip was used as a reference sample, while a gold thin film (50 nm thickness) and a gold nanorod-based metamaterial with and without alumina (see SEM image, Figure 1a), allowing the D-A pairs to be located inside and on top of the metamaterial, were considered. A free-standing polymer coated gold nanorod-based metamaterial was also investigated to limit quenching of the emission for pairs located close to each individual nanorod. Figure 1 depicts the different environments used.

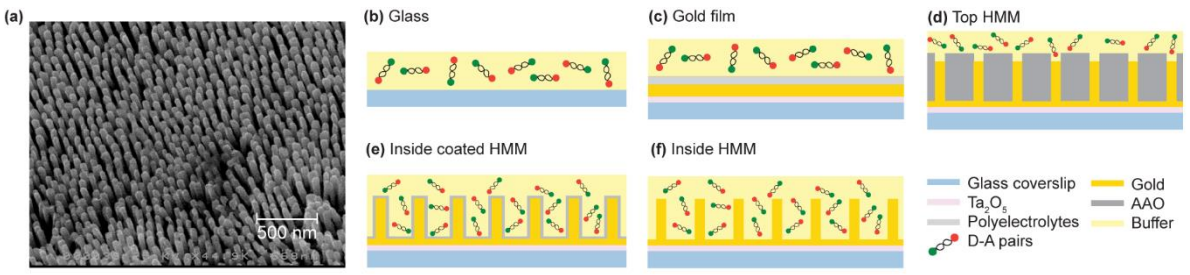


**Figure 1. Material environments. (a)** SEM image of the free-standing nanorod-based hyperbolic metamaterial (tilted at 30°). **(b-f)** Different material environments used in this

experimental study. The D-A pairs were deposited (b) on a glass coverslip, (c) on a 50 nm thick gold film, (d) on top of the nanorod-based hyperbolic metamaterial, (e) inside the nanorod-based metamaterial coated with a 7.5 nm thick layer of polyelectrolytes and (f) inside the bare nanorod-based metamaterial.

The nanorod-based metamaterials were fabricated by gold electrodeposition into highly ordered nanoporous alumina templates on glass coverslips, following the method described in Ref. 26. The geometrical parameters of the nanorod arrays used in the experiments were approximately 50 ± 2 nm rod diameter, 100 ± 2 nm inter-rod spacing and 260 ± 5 nm rod height. The alumina surrounding the gold nanorods was subsequently dissolved in order to obtain free-standing nanorods. Figure 2a shows the optical properties of the free-standing gold nanorods in the water-based annealing buffer in which the D-A pairs were suspended. The real part of the permittivity component along the nanorods ($\varepsilon_{zz}$) becomes negative around 580 nm, corresponding to the characteristic epsilon-near-zero (ENZ) range of the metamaterial (Figure 2c). The metamaterial therefore operates in the hyperbolic regime of dispersion for wavelengths above 580 nm, coinciding with the region of spectral overlap of the donor and acceptor (Figure S1).

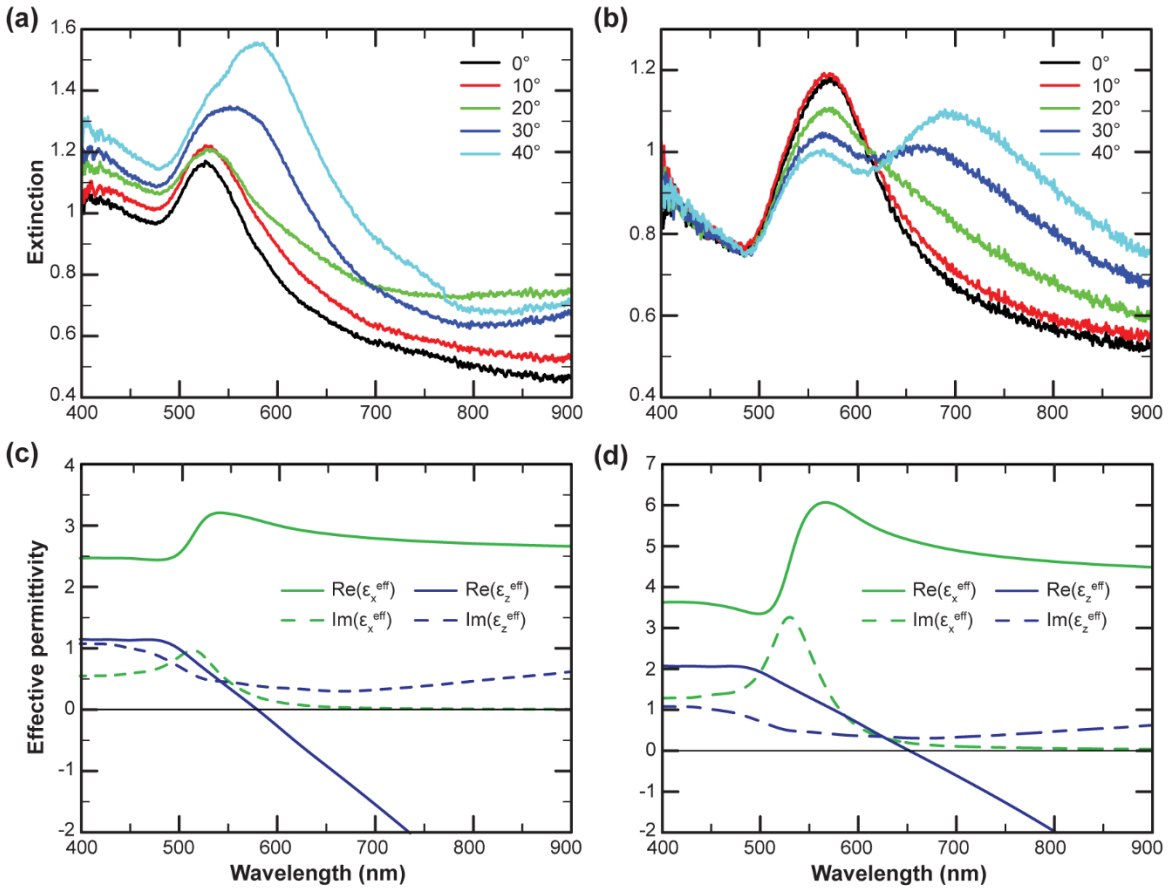


**Figure 2. Experimental extinction spectra (-logT) of the gold nanorod-based hyperbolic metamaterial in different host environments and effective permittivities modelled using an EMT. (a, b)** Experimental extinction spectra of the metamaterial (a) in water-based annealing buffer and **(b)** embedded in alumina. The measurements were taken for different angles of incidence of TM-polarised light. **(c, d)** Spectra of the real (Re) and imaginary (Im) parts of the principal components of the effective permittivity tensor of the metamaterial with nanorods in (c) water-based buffer and (d) embedded in alumina.

An additional sample was then fabricated in order to study the energy transfer for D-A pairs located on top of the metamaterial. This sample was made with the same geometrical parameters as the free-standing gold nanorods sample described above but kept in the alumina

matrix (Figure 2b). Due to the fabrication process, the gold nanorods are recessed below the surface of the porous alumina matrix, as depicted in Figure 1d. While in this case the spectral overlap of the donor and acceptor mostly lies in the elliptic dispersion regime of the metamaterial, the spectral proximity of the ENZ region is still expected to influence the FRET process, as was also confirmed for the Purcell effect (20).

In order to coat the gold nanorod-based metamaterial with a thin layer of polymer, a new sample was used. The geometrical parameters of the nanorods were estimated as 52 ± 2 nm rod diameter, 100 ± 2 nm inter-rod spacing and 127 ± 5 nm rod height. The coating of the gold nanorod sample with a thin layer of polymer (7.5 nm) to prevent quenching was performed using a layer-by-layer deposition technique as described in the Methods section. Figure S2a depicts the extinction spectra of the coated nanorod sample in air for different angles of incidence for TM-polarised light.

As expected, the extinction peaks strongly depend on the nanorod environment, with the structure exhibiting two peaks associated with electron motion parallel and perpendicular to the nanorods. While these two modes overlap in the case where the gold nanorods are surrounded with air (Figure S2b), an increased splitting is observed in environments of higher refractive indices.

***Time-resolved photoluminescence and Laplace transform analysis.*** The FRET rate modification together with the LDOS enhancement in the different environments were evaluated by recording the decay dynamics of the donor, for different D-A separations, using a time-correlated single photon counting (TCSPC) technique. The emission decays were then analysed using an inverse Laplace transform method as described in the Methods section. Figure 3(a,c,e,g,i) reports the normalised decay curves for the various environments. In the

case of the donor alone, the lifetime of the donor is decreased by the presence of the gold film and the metamaterial samples, corresponding to an increase in the decay rate of the donor $\Gamma_D = 1/\tau_D$ and revealing the modification of the LDOS for each environment. Evidence of the energy transfer between the donor and the acceptor is provided by the further reduction of the donor's lifetime in the presence of the acceptor, to $\tau_{DA} = 1/\Gamma_{DA}$ for each D-A separation, due to the additional decay channel for energy transfer between the donor and the acceptor.

From the fluorescence decays and lifetime distributions (Figure 3), one can see that while a mono-exponential decay of fluorescence and narrow lifetime distribution (Figure 3a,b) are observed in the case of the donors alone deposited on glass, both the presence of the acceptor and the modification of the environment surrounding the D-A pairs significantly influence the decay dynamics of the donor. In the presence of the acceptor and, therefore, an additional decay channel, the lifetime distributions of the donor on glass exhibit a slight shift towards shorter lifetimes together with only a slight broadening of lifetime distribution, leading to the almost single exponential decays observed in Figure 3a. However, when located near a plasmonic environment, the fluorescence decay curves of the donor and their corresponding lifetime distributions become more complex, especially in the case of the D-A pairs placed inside the bare HMM. The decay dynamics of the donor alone inside the bare HMM, averaged over the ensemble, is strongly accelerated, reflecting a strong dependence of the decay rate on the distance and orientation of the molecules with regard to the surrounding nanorods (as was shown in Ref. 20). The random positions of the molecules as well as the random orientations of their dipole moments within the environment lead to a broadened lifetime distribution dominated by short lifetime contributions, accompanied by smaller contributions of longer lifetimes represented by the low amplitude tail (Figure 3f). This ultimately leads to a multi-exponential profile of the decay dynamics. With the addition of the acceptor, the donor lifetime distributions inside the bare HMM are further shifted towards shorter lifetimes. As for the other

systems, including the molecules located on top of the gold film thinly coated with PMMA or on top of the HMM in its alumina matrix, as well as the HMM constituted of coated nanorods, the modification of the decay rate is generally more moderate. Nevertheless, the decay dynamics of the donor in all cases become strongly multi-exponential with the decrease in D-A distance.

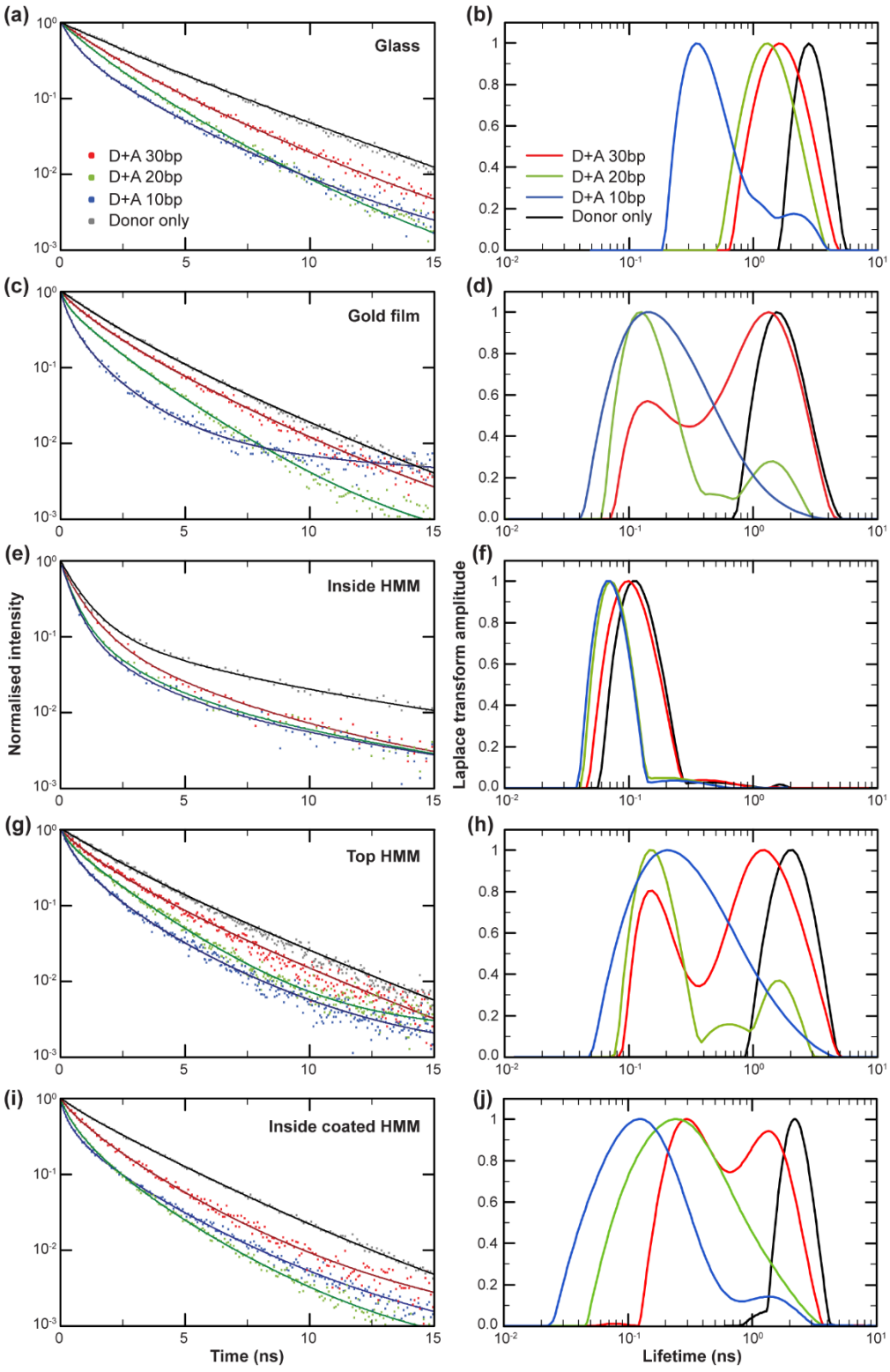


**Figure 3. Normalised decay dynamics of the donor for different donor-acceptor separations in different environments (a,c,e,g,i) and Laplace analysis (b,d,f,h,j).** (a, b) On glass, (c,d) on a 50 nm thick gold film, (e,f) inside the gold nanorod-based metamaterial, (g,h)

on top of the gold nanorod-based metamaterial, (i,j) inside the polymer coated gold nanorod-based metamaterial.

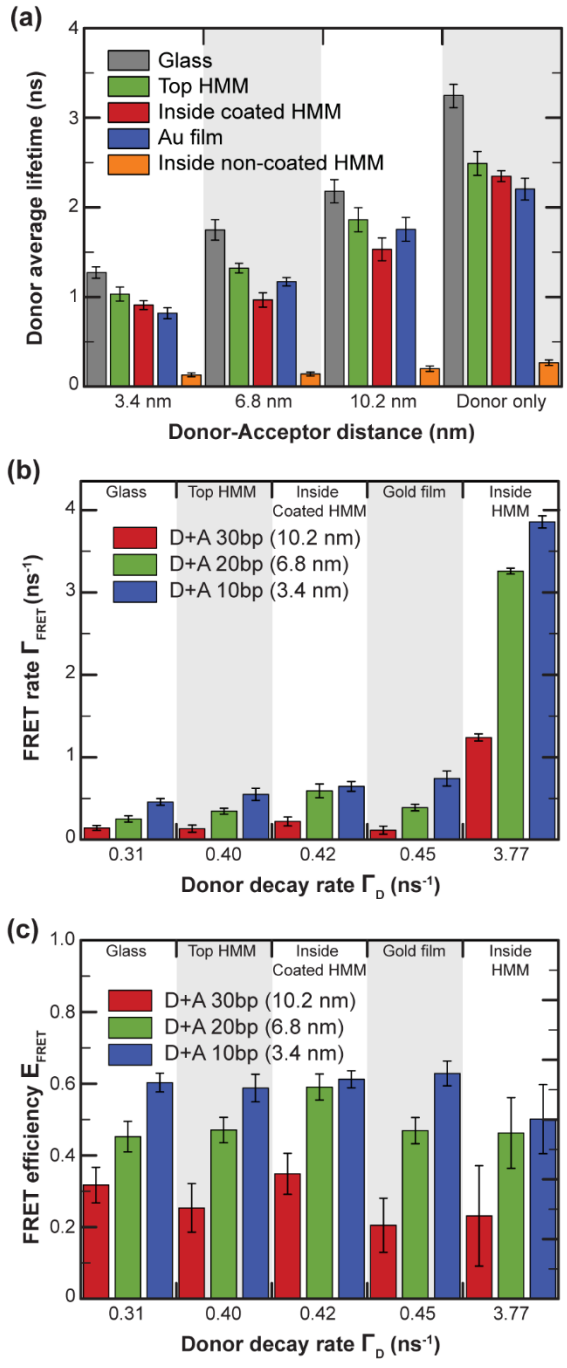


**Figure 4. Decay dynamics and lifetime distribution analysis.** (a) Average lifetime of the donor in different electromagnetic environments as a function of the D-A separation. (b) FRET

rates and (c) FRET efficiencies for different electromagnetic environments as a function of the increase in local density of states (LDOS).

***FRET rates and efficiencies.*** The decay rate of the donor within a given environment can be expressed as a function of the decay rate of the donor alone $\Gamma_D$ and the energy transfer rate $\Gamma_{FRET}$, such that $\Gamma_{DA} = \Gamma_D + \Gamma_{FRET}$. While this relation is derived for a single D-A pair, in the presence of an ensemble of D-A pairs with different orientations relative to the nanorods, the respective rates should be considered as averaged over all possible orientations.

In order to evaluate the modification of the FRET rate and FRET efficiency in the different environments, the lifetime distributions, obtained by the inverse Laplace transform analysis of the emission dynamics of the donor in each environment, were used to calculate an amplitude-averaged lifetime defined by $\langle\tau\rangle = \int_0^\infty \alpha_i d\tau_i$, where $\tau_i$ is the lifetime component of the donor and $\alpha_i$ its corresponding amplitude (27). From Figure 4a, an average lifetime of approx. 3.2 ± 0.2 ns is observed in the case of the donor alone on a glass substrate, which is consistent with the value reported in the literature (28). In all other cases, the average lifetimes are reduced, especially for the D-A pairs inside the bare HMM, reaching a few hundreds of picoseconds. The more moderate decrease of the average lifetimes in the remaining environments can be related to a smaller contribution of the short lifetime component of the distribution, compared to the case of the bare HMM.

From these average lifetimes, averaged over all locations and all orientations, the rate $\Gamma_{FRET}$ and efficiency $E_{FRET}$ of energy transfer were calculated using equations 5 and 6, as described in the Methods section. In order to evaluate the influence of the LDOS on the energy transfer, the FRET rates and efficiencies were represented in Figure 4b,c as a function of the decay rate of the donor alone in different environments, representing the modification of the

LDOS. From the values of the donor decay rate given in Figure 4b, the increase in the LDOS from the glass substrate to the top of the metamaterial and the gold film is moderate, with rates increasing from 0.31 $ns^{-1}$ to 0.40 $ns^{-1}$ and 0.45 $ns^{-1}$, respectively, corresponding to enhancements of 1.3-fold and 1.45-fold. The same observation was made in the case of the polymer coated nanorod-based metamaterial, where the decay rate of the donor is equal to 0.42 $ns^{-1}$ (1.35-fold enhancement). In the case of the D-A pairs located inside the bare metamaterial, the increase of the decay rate of the donor is more significant, from 0.31 $ns^{-1}$ to 3.77 $ns^{-1}$, corresponding to a LDOS enhancement of 12-fold. This increase of the decay rate of the donor inside the bare metamaterial arises from a strong dependence of the spontaneous emission properties on the position of the D-A pairs with regard to the adjacent nanorods and their local fields (29). For all separations between donor and acceptor, the FRET rate was found to increase linearly with the LDOS. An increase reaching up to 13-fold was measured for D-A pairs located inside the bare metamaterial. The non-trivial behaviour of the FRET characteristics in the complex environments studied could also have been related to various other factors. The study of an ensemble of D-A pairs rather than single pairs has been shown to lead to collective effects or cross-talk between FRET pairs, playing an important role in the energy transfer process, as described in several studies (25,30). To ensure the concentration used for all measurements is low enough so these effects are negligible in our study, the decay dynamics of the donor were measured at three different concentrations of D-A pairs. For each D-A separation, all three decay dynamics have been shown to be identical, confirming the low influence of these effects on the experimental results (see Figure S3). Other factors such as inaccurate pairing of the D-A pairs, leading to different distances between donors and acceptors could also influence the experimental results.

Using the donor decay dynamics observed above and equation 6, FRET efficiencies were calculated for the three separations between the donor and the acceptor in each environment.

As observed from Figure 4c, a separation of 3.4 nm (10 base pairs) between the donor and the acceptor led to a measured FRET efficiency of about 60% on glass, while a FRET efficiency of about 47 % and 30 % were measured for separations of 6.8 nm and 10.2 nm, respectively. Our analysis reveals that in most cases, FRET efficiencies show only slight variations with the increase in LDOS. These small variations are consistent with an increase of the FRET rate as increasing the donor decay rate for each environment and keeping the efficiency constant requires the FRET rate to increase[14], as shown in Eq. 5-6. This study of FRET through time-resolved analysis of the emission dynamics of the donor has revealed no significant dependence of the FRET efficiency on material environment but has shown a linear increase of the FRET rate with the LDOS, most pronounced inside the metamaterial. Interestingly, FRET observed in the vicinity of hyperbolic metamaterials constructed with metal-dielectric multilayers shows inhibition of the FRET rate (25). The latter has been explained by possible collective dye-plasmon interactions, present in the case of concentrated enough molecular ensembles. These collective effects have however been ruled out our experimental study performed at lower concentrations.

***Free-space donor-acceptor emission intensity.*** The manifestation of FRET in D-A pairs located in different environments can also be explored via the study of the relative emission intensity between the donor and the acceptor. Here the intensity of the acceptor free-space emission collected through the substrate was recorded and normalised to the peak emission intensity of the donor. The direct emission intensity of the acceptor at the excitation wavelength of the donor, measured separately for each material environment, was subtracted beforehand. Figure 5 depicts the results obtained where the energy transfer generally manifests itself by the increase of acceptor emission intensity for shorter separations between the donor and the acceptor.

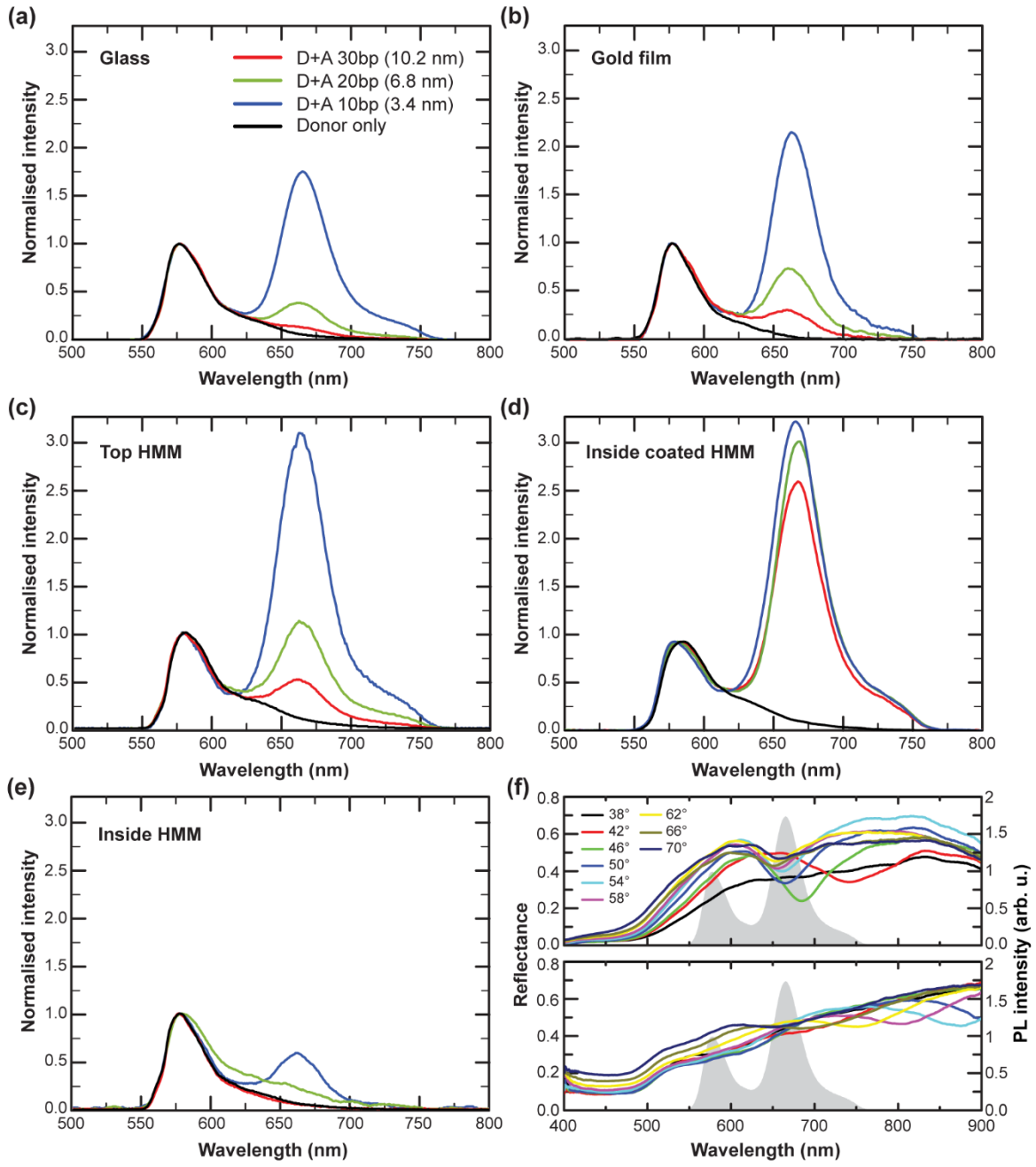


**Figure 5. Free-space D-A emission intensity for different D-A separations in different environments and reflection spectra. (a-e)** Free-space D-A emission intensity for different D-A separations (a) on glass, (b) on a 50 nm thick gold film, (c) on top of the gold nanorod-based metamaterial, (d) inside the polymer coated gold nanorod-based metamaterial, (e) inside the bare gold nanorod-based metamaterial. The data were normalised to the peak emission intensity of the donor. **(f)** Experimental attenuated total reflection (ATR) measurements of the

bare (top panel) and coated (bottom panel) nanorod-based hyperbolic metamaterial for TM polarisation. The embedding material surrounding the nanorods is a water-based annealing buffer. The greyed area represents the free-space emission spectrum of the donor and acceptor.

Compared to the D-A pairs placed on glass (Figure 5a), the acceptor emission intensities in the case of the gold film and on top of the metamaterial are both increased (Figure 5b,c) whereas in the case of molecules inside the bare metamaterial, the emission intensity is greatly reduced for all separations (Figure 5e). According to the study reported in Ref. 21, the reduced free-space emission of the acceptor can be due to the coupling of the emitted light to the waveguided mode supported by the structure. In order to verify this hypothesis, the dispersion of reflection for TM-polarised waves was measured for both bare and coated metamaterial embedded in annealing buffer. Figure 5f (top panel) shows that one of the TM-polarised waveguided modes supported by the bare metamaterial structure overlaps significantly with the emission of the acceptor, thus favouring the coupling of the acceptor emission to this mode. Photoluminescence measurements were then performed on the polymer coated free-standing gold nanorod-based metamaterial as shown in Figure 5d. It is shown that the free-space intensity of the acceptor is largely enhanced for all D-A separations. In this case, the presence of the coating around the nanorods acts as a spacer between the metal and the dye molecules in order to avoid quenching but also contributes, together with the geometrical properties of the sample, to the modification of the optical properties of the material, thus altering its mode structure. This therefore affects the position of the waveguided modes of the metamaterial and in this case does not prevent the free-space emission of the acceptor, as there is no significant overlap between the emission of the dye and the modes supported by the structure (Figure 5f - bottom panel). An increase of the free-space emission intensity of the acceptor inside the coated HMM reaching up to 18-fold has been observed for larger D-A separations.

## Conclusion

We have investigated the energy transfer between a donor and an acceptor fluorophores with precise separations located in different electromagnetic environments. In most environments with increased LDOS, an increase in the donor spontaneous emission rate as well as the FRET rate were observed, in comparison to the rates of emitters placed on glass. In particular, D-A pairs placed inside the gold nanorod-based metamaterial, showing a 12-fold increase of the LDOS, exhibited a 13-fold increase of the FRET rate along with only slight variations of the FRET efficiency compared to those located on glass. The free-space intensity measurements of the acceptor emission for D-A pairs inside the metamaterial also revealed a strong decrease in the acceptor emission attributed to the coupling of the emission to the waveguided mode supported by the system at the emission wavelength of the acceptor. For the emitters located on top of a gold film, on top of the nanorod-based metamaterial or inside the polymer coated metamaterial, the increases in the decay rates of the donor as well as the FRET rates remained moderate, and the free-space emission of the acceptor normalised to the donor emission increased in all cases compared to the emission intensity on glass. The highest increase in intensity was observed in the case of the polymer coated metamaterial. The coating of the nanorod-based metamaterial with a thin polymer layer has shown to be a good solution to avoid quenching but also strongly reduces the decay rates compared to the emitters located inside the bare metamaterial, for which the small separations between the fluorophores and the nanorods have a strong effect on the emission rate (20). The homogeneity of the coating still remains a challenge and needs to be improved for future experiments. This could potentially be achieved by functionalising the gold nanorods with thiols of fixed lengths in order to avoid multi-step deposition processes. These results show the potential of highly tunable hyperbolic

metamaterial for the control of the energy transfer between emitters and the design of fast and enhanced light-emitting devices.

## Methods

***Donor-acceptor pairs.*** For this study, D-A pairs are constituted of ATTO 550 and ATTO 647N molecules. These dyes typically exhibit strong absorption ($\varepsilon_{ATTO550}=1.2\times10^5$ $M^{-1}.cm^{-1}$ at 554 nm; $\varepsilon_{ATTO647N}=1.5\times10^5$ $M^{-1}.cm^{-1}$ at 644 nm), high fluorescence quantum yield ($Q_{ATTO550}=0.80$; $Q_{ATTO647N}=0.65$) and high photostability. As presented in Figure S1, the normalised emission spectrum of the donor and the normalised absorption spectrum of the acceptor show a spectral overlap which is one of the key conditions for FRET to occur. The Förster radius, $R_0$, for these two molecules freely suspended in water is equal to 6.5 nm, assuming dynamic random averaging of the donor and the acceptor ($\kappa=2/3$). In order to control the separation between donor and acceptor, the emitters were attached to complementary single-stranded DNA oligonucleotides (Eurofins Genomics) of known lengths and then hybridised. Three different lengths of DNA strands were used: 10, 20 and 30 base pairs respectively corresponding to 3.4 nm, 6.8 nm and 10.2 nm, providing three different FRET efficiencies. Prior to hybridisation, the complementary oligonucleotides were suspended at the same molar concentration (100 $\mu mol.L^{-1}$) in a water-based annealing buffer composed of 10 $mmol.L^{-1}$ Tris-HCL, 1 $mmol.L^{-1}$ EDTA and 30 $mmol.L^{-1}$ NaCl. The pH of the solution was then adjusted to 7.85 with NaOH. Equal volumes of both complementary strands were then mixed and heated at 90°C for 5 minutes and cooled to room temperature for an hour. Prior to the measurements, the emitters solutions were diluted 100 times to a final concentration of 1 $\mu mol.L^{-1}$.

***Fabrication of the metamaterial.*** The nanorod-based hyperbolic metamaterials were fabricated by electrodepositing gold into a porous alumina template, following the method described in Ref. 26. In the case of the bare and polymer coated samples, the alumina matrix was removed using a solution of 0.3M NaOH and 99.5% ethanol. The polymer coated nanorod sample was then prepared using a layer-by-layer deposition of polyelectrolytes (31). Each polyelectrolyte layer was prepared by alternating the deposition of poly(allylamine hydrochloride) and polystyrene sulfonate. For each deposition step, the plasmonic gold nanorod metamaterial was immersed in a polyelectrolyte solution (10 $mg.mL^{-1}$ in 1 $mmol.L^{-1}$ NaCl aqueous solution) for 30 minutes and washed with pure water (18 MΩ) to remove any unbound electrolyte. The layer-by-layer process was initiated with the cationic poly(allylamine hydrochloride) layer in order to facilitate the attachment of the first polyelectrolyte layer to the gold nanorods through amine-gold interactions. The thickness of the deposited polyelectrolyte layer was measured by TEM on a sacrificial sample. The nanorods were pulled off the substrate by sonication and subsequently covered with gold nanoparticles (2-3 nm diameter) in order to visualise the gap between the nanorods and the gold nanoparticles. To perform the measurements, 0.5 μL of solution was drop casted on the different samples.

***Optical characterisation.*** Transmission measurements were taken using a tungsten-halogen lamp for varying polarisations and angles of incidence on the sample. The light was collimated onto the sample from the substrate side and the transmitted light collected by an objective lens. The transmitted light is then coupled to a spectrometer equipped with a CCD camera via a multimode optical fibre. An attenuated total reflection (ATR) configuration was used for the detection of the waveguided modes, not available from free-space. In this case, the sample was placed in contact with a glass semi-cylinder and was illuminated through it.

***Time-resolved photoluminescence measurements.*** Time-resolved photoluminescence measurements were carried out using time-correlated single photon counting (TCSPC). A laser beam from a supercontinuum laser (20 MHz repetition rate, 400 fs pulse, 0.4 mW), filtered with a 10 nm bandpass filter centered on 532 nm, was focused on the sample using a high-numerical aperture oil-immersion objective (100x, NA = 1.49) and the PL signal was collected via the same objective. Different sets of filters were used in order to record the decay dynamics of both the donor (bandpass 575/40 nm) and the acceptor (bandpass 705/72 nm), and also remove the laser contribution to the measured signal (Notch filter 532 nm and longpass >550 nm filter).

***Theoretical FRET Analysis.*** Considering a single donor and acceptor separated by a distance $r$, the rate of energy transfer $\Gamma_{FRET}(r)$ is given by

$$\Gamma_{FRET}(r) = \left(\frac{9000 \ln 10}{128\pi^5 N_A n^4}\right) J(\lambda) \frac{Q_D \kappa^2}{\tau_D r^6} \qquad (1)$$

where $n$ is the refractive index of the medium in which the D-A pairs are suspended and $N_A$ is Avogadro's number. The term $J(\lambda)$ in equation 1 is an overlap integral, representing the spectral overlap between the donor emission and the acceptor absorption spectra, and is defined as

$$J(\lambda) = \int_0^\infty F_D(\lambda)\epsilon_A(\lambda)\lambda^4 \, d\lambda \qquad (2)$$

where $F_D(\lambda)$ is the donor emission spectrum normalised to an area of 1, $\epsilon_A(\lambda)$ is the molar extinction coefficient of the acceptor (in units of $mol^{-1}.cm^{-1}$) and $\lambda$ is the wavelength of light (in nm). $Q_D$ is the quantum yield of the donor in the absence of the acceptor, $\tau_D$ is the lifetime of the donor in the absence of the acceptor and $\kappa^2$ is an orientation factor describing the relative

orientation of the transition dipole moments of the donor and the acceptor. Depending on the relative orientation of the donor and acceptor dipole moments, $\kappa^2$ can take values between 0 and 4. In the case of dynamic random averaging by rotational diffusion of the donor and acceptor, $\kappa^2$ is usually assumed to be equal to 2/3. However, this value can change in the case of static averaging, for which the orientation between donor and acceptor is constrained or does not change during the excited-state lifetime (32). The presence of DNA linkers between the donor and the acceptor, as used in this study, has been shown to influence the value of $\kappa^2$ and its theoretical determination, specific to each D-A pair, requires the study of the molecular binding of the system (33,34). In the case of dynamic random averaging of the donor and acceptor in uniform electromagnetic environment, equation 3 can then be expressed in terms of the Förster radius $R_0$, corresponding to the distance at which the probabilities of spontaneous decay of the excited donor and energy transfer are equal, yielding

$$\Gamma_{FRET}(r) = \frac{1}{\tau_D}\left(\frac{R_0}{r}\right)^6 \qquad (3)$$

In other words, $R_0$ is the distance between the donor and acceptor at which the efficiency of energy transfer is equal to 50 %, leading to the following expression of the FRET efficiency

$$E_{FRET} = \frac{1}{1+\left(\frac{r}{R_0}\right)^6} \qquad (4)$$

When located in a plasmonic environment, the energy transfer between the donor and acceptor can be affected by multiple factors. Both the relative orientation of the donor and acceptor dipole moments with regard to the plasmonic environment and the respective distance of the donor and acceptor to the plasmonic nanorods contribute to a modified FRET rate and efficiency, averaged over all positions and orientations of the D-A pairs. In this study, the FRET rate ($\Gamma_{\mathrm{FRET}}$) and efficiency ($\mathrm{E_{FRET}}$) have been calculated solely from the lifetimes of the donor in absence ($\Gamma_D$) and presence ($\Gamma_{DA}$) of the acceptor, using the following equations

$$\Gamma_{FRET} = \Gamma_{DA} - \Gamma_D = \frac{1}{\tau_{DA}} - \frac{1}{\tau_D} \qquad (5)$$

$$E_{FRET} = 1 - \frac{\Gamma_D}{\Gamma_{DA}} = 1 - \frac{\tau_{DA}}{\tau_D} \qquad (6)$$

***Fluorescence lifetime data analysis.*** Time-resolved measurements were analysed using an inverse Laplace transform method (20,35), allowing the determination of lifetime distributions of the donor in the absence and presence of the acceptor. This method does not require any preliminary estimation of the lifetime distribution and is based on the solution of the equation

$$I(t) = \int_0^\infty F(\tau) e^{-t/\tau} d\tau \qquad (7)$$

where $I(t)$ is the measured decay deconvoluted from the instrumental response function and $F(\tau)$ is the relative weight of the exponential decay components. In order to account for the noise in the experimental fluorescence decays and thus the ill-defined character of inverse methods, a constrained regularization procedure was implemented (35,36) and an iterative fitting was performed to obtain stable results..

***EMT modelling.*** The optical properties of the metamaterial were modelled using an effective medium theory (EMT) based on Maxwell-Garnett approximation (37). The in-plane (*xy*-directions) and out of plane (*z*-direction) components of the effective dielectric permittivity are expressed as

$$\epsilon_{xy}^{eff} = \epsilon_h \frac{(1+p)\epsilon_{Au} + (1-p)\epsilon_h}{(1-p)\epsilon_{Au} + (1+p)\epsilon_h} \qquad (8)$$

$$\epsilon_z^{eff} = p\epsilon_{Au} + (1-p)\epsilon_h \qquad (9)$$

where $p = \pi(r/d)^2$ is the nanorod concentration with $r$ the radius of the nanorods and $d$ the distance between the nanorods. $\epsilon_{Au}$ and $\epsilon_h$ are the permittivities of gold and the host medium, respectively. This model is valid away from the Brillouin zone edge of the nanorod array.

## ASSOCIATED CONTENT

### Supporting Information

The Supporting Information is available free of charge on the ACS publication website.

Absorption and emission spectra of ATTO 550 and ATTO 647N dyes, Experimental extinction spectra of the gold nanorod-based hyperbolic metamaterial in different host environments, Normalised decay dynamics of the donor for different donor-acceptor concentrations and separations on glass.

## AUTHOR INFORMATION


### Corresponding Author

* E-mail: diane.roth@kcl.ac.uk


### Author Contributions

The manuscript was written through contributions of all authors. All authors have given approval to the final version of the manuscript.

### Notes

The authors declare no competing financial interest.

## ACKNOWLEDGMENTS

This work has been funded in part by the Engineering and Physical Sciences Research Council (UK) and the European Research Council iPLASMM project (321268). A.Z. acknowledges support from the Royal Society and the Wolfson Foundation. The data access statement: all data supporting this research are provided in full in the results section and Supporting Information.

## *References*

1. Förster, T. Energiewanderung und fluoreszenz. *Naturwissenschaften* **1946,** *33*, 166-175. (Translated by Suhling, K. Energy migration and fluorescence. *J. Biomed. Opt.* **2012**, 17, 011002.)
2. Förster, T. Zwischenmolekulare energiewanderung und fluoreszenz. *Ann. Phys.* **1948,** *437*, 55-75. (Translated by Knox, R.S. Intermolecular energy migration and fluorescence. In *Biological Physics*; Mielczarek, E.V., Greenbaum, E., Knox, R.S., Eds.; American Institute of Physics: New York, 1993; pp 148-160.)
3. Kenworthy, A. K. Imaging protein-protein interactions using fluorescence resonance energy transfer microscopy. *Methods* **2001,** *24*, 289-296.
4. Jares-Erijman, E. A.; Jovin, T. M. FRET imaging. *Nat. Biotechnol.* **2003,** *21*, 1387.
5. Kalinin, S.; Peulen, T.; Sindbert, S.; Rothwell, P. J.; Berger, S.; Restle, T.; Goody, R. S.; Gohlke, H.; Seidel, C. A. A toolkit and benchmark study for FRET-restrained high-precision structural modeling. *Nat. Methods* **2012,** *9*, 1218.
6. Hardin, B. E.; Hoke, E. T.; Armstrong, P. B.; Yum, J.-H.; Comte, P.; Torres, T.; Fréchet, J. M.; Nazeeruddin, M. K.; Grätzel, M.; McGehee, M. D. Increased light harvesting in dye-sensitized solar cells with energy relay dyes. *Nat. Photonics* **2009,** *3*, 406.
7. Baldo, M.; Thompson, M.; Forrest, S. High-efficiency fluorescent organic light-emitting devices using a phosphorescent sensitizer. *Nature* **2000,** *403*, 750.
8. Brovelli, S.; Meinardi, F.; Winroth, G.; Fenwick, O.; Sforazzini, G.; Frampton, M. J.; Zalewski, L.; Levitt, J. A.; Marinello, F.; Schiavuta, P., Suhling, K.; Anderson, H. L.; Cacialli, F. White Electroluminescence by Supramolecular Control of Energy Transfer in Blends of Organic-Soluble Encapsulated Polyfluorenes. *Adv. Funct. Mater.* **2010,** *20* , 272-280.
9. Blum, C.; Zijlstra, N.; Lagendijk, A.; Wubs, M.; Mosk, A. P.; Subramaniam, V.; Vos, W. L. Nanophotonic control of the Förster resonance energy transfer efficiency. *Phys. Rev. Lett.* **2012,** *109*, 203601.
10. Andrew, P.; Barnes, W. L. Förster energy transfer in an optical microcavity. *Science* **2000,** *290*, 785-788.
11. Zhang, X.; Marocico, C. A.; Lunz, M.; Gerard, V. A.; Gun'ko, Y. K.; Lesnyak, V.; Gaponik, N.; Susha, A. S.; Rogach, A. L.; Bradley, A. L. Experimental and theoretical investigation of the distance dependence of localized surface plasmon coupled Forster resonance energy transfer. *ACS Nano* **2014,** *8*, 1273-1283.
12. Ghenuche, P.; Mivelle, M.; de Torres, J.; Moparthi, S. B.; Rigneault, H.; Van Hulst, N. F.; García-Parajó, M. F.; Wenger, J. Matching nanoantenna field confinement to FRET distances enhances forster energy transfer rates. *Nano Lett.* **2015,** *15*, 6193-6201.
13. Bidault, S. b.; Devilez, A.; Ghenuche, P.; Stout, B.; Bonod, N.; Wenger, J. Competition between Förster Resonance Energy Transfer and Donor Photodynamics in Plasmonic Dimer Nanoantennas. *ACS Photonics* **2016,** *3*, 895-903.

14. Ghenuche, P.; de Torres, J.; Moparthi, S. B.; Grigoriev, V.; Wenger, J. Nanophotonic enhancement of the Forster resonance energy-transfer rate with single nanoapertures. *Nano Lett.* **2014,** *14*, 4707-14.
15. Dung, H. T.; Knöll, L.; Welsch, D.-G. Intermolecular energy transfer in the presence of dispersing and absorbing media. *Phys. Rev. A* **2002,** *65*, 043813.
16. Cortes, C. L.; Jacob, Z. Fundamental figures of merit for engineering Förster resonance energy transfer. *Opt. Express* **2018**, 26, 19371-19387.
17. Nakamura, T.; Fujii, M.; Miura, S.; Inui, M.; Hayashi, S. Enhancement and suppression of energy transfer from Si nanocrystals to Er ions through a control of the photonic mode density. *Phys. Rev. B* **2006,** *74*, 045302.
18. De Dood, M.; Knoester, J.; Tip, A.; Polman, A. Förster transfer and the local optical density of states in erbium-doped silica. *Phys. Rev. B* **2005,** *71*, 115102.
19. Lu, D.; Kan, J. J.; Fullerton, E. E.; Liu, Z. W. Enhancing spontaneous emission rates of molecules using nanopatterned multilayer hyperbolic metamaterials. *Nat. Nanotechnol.* **2014,** *9*, 48-53.
20. Ginzburg, P.; Roth, D. J.; Nasir, M. E.; Segovia, P.; Krasavin, A. V.; Levitt, J.; Hirvonen, L. M.; Wells, B.; Suhling, K.; Richards, D.; Podolskiy, V. A.; Zayats, A. V. Spontaneous emission in non-local materials. *Light: Sci. Appl.* **2017,** *6*, e16273.
21. Roth, D. J.; Krasavin, A. V.; Wade, A.; Dickson, W.; Murphy, A.; Kéna-Cohen, S.; Pollard, R.; Wurtz, G. A.; Richards, D.; Maier, S. A.; Zayats, A. V. Spontaneous emission inside a hyperbolic metamaterial waveguide. *ACS Photonics* **2017,** *4*, 2513-2521.
22. Krishnamoorthy, H. N.; Jacob, Z.; Narimanov, E.; Kretzschmar, I.; Menon, V. M. Topological transitions in metamaterials. *Science* **2012,** *336*, 205-209.
23. Kabashin, A.; Evans, P.; Pastkovsky, S.; Hendren, W.; Wurtz, G.; Atkinson, R.; Pollard, R.; Podolskiy, V.; Zayats, A. V. Plasmonic nanorod metamaterials for biosensing. *Nat. Mater.* **2009,** *8*, 867.
24. Narimanov, E. E.; Kildishev, A. V. Metamaterials: naturally hyperbolic. *Nat. Photonics* **2015,** *9*, 214.
25. Tumkur, T. U.; Kitur, J. K.; Bonner, C. E.; Poddubny, A. N.; Narimanov, E. E.; Noginov, M. A. Control of Förster energy transfer in the vicinity of metallic surfaces and hyperbolic metamaterials. *Faraday Discuss.* **2015,** *178*, 395-412.
26. Evans, P.; Hendren, W.; Atkinson, R.; Wurtz, G.; Dickson, W.; Zayats, A. V.; Pollard, R. Growth and properties of gold and nickel nanorods in thin film alumina. *Nanotechnology* **2006,** *17*, 5746.
27. Sillen, A.; Engelborghs, Y. The correct use of “average” fluorescence parameters. *Photochem. Photobiol.* **1998,** *67*, 475-486.
28. ATTO-TEC Catalog. https://www.atto-tec.com/fileadmin/user_upload/Katalog_Flyer_Support/Katalog_2016_2018.pdf (accessed Jul 19, 2018)
29. Slobozhanyuk, A. P.; Ginzburg, P.; Powell, D. A.; Iorsh, I.; Shalin, A. S.; Segovia, P.; Krasavin, A. V.; Wurtz, G. A.; Podolskiy, V. A.; Belov, P. A.; Zayats, A. V. Purcell effect in hyperbolic metamaterial resonators. *Phys. Rev. B* **2015,** *92*, 195127.
30. Poddubny, A. N. Collective Förster energy transfer modified by a planar metallic mirror. *Phys. Rev. B* **2015,** *92*, 155418.
31. Ciracì, C.; Hill, R.; Mock, J.; Urzhumov, Y.; Fernández-Domínguez, A.; Maier, S.; Pendry, J.; Chilkoti, A.; Smith, D. Probing the ultimate limits of plasmonic enhancement. *Science* **2012,** *337*, 1072-1074.
32. Vogel, S. S.; Nguyen, T. A.; van der Meer, B. W.; Blank, P. S. The impact of heterogeneity and dark acceptor states on FRET: implications for using fluorescent protein donors and acceptors. *PLoS One* **2012,** *7*, e49593.
33. de Torres, J.; Mivelle, M.; Moparthi, S. B.; Rigneault, H.; Van Hulst, N. F.; García-Parajó, M. F.; Margeat, E.; Wenger, J. Plasmonic Nanoantennas Enable Forbidden Förster Dipole–Dipole Energy Transfer and Enhance the FRET Efficiency. *Nano Lett.* **2016,** *16*, 6222-6230.

34. Iqbal, A.; Arslan, S.; Okumus, B.; Wilson, T. J.; Giraud, G.; Norman, D. G.; Ha, T.; Lilley, D. M. Orientation dependence in fluorescent energy transfer between Cy3 and Cy5 terminally attached to double-stranded nucleic acids. *Proc. Natl. Acad. Sci. U. S. A.* **2008,** *105*, 11176-11181.
35. Provencher, S. W. Inverse problems in polymer characterization: direct analysis of polydispersity with photon correlation spectroscopy. *Macromol. Chem. Phys.* **1979,** *180*, 201-209.
36. Provencher, S. W. A constrained regularization method for inverting data represented by linear algebraic or integral equations. *Comput. Phys. Commun.* **1982,** *27*, 213-227.
37. Elser, J.; Wangberg, R.; Podolskiy, V. A.; Narimanov, E. E. Nanowire metamaterials with extreme optical anisotropy. *Appl. Phys. Lett.* **2006,** *89*, 261102.

**For Table of Contents Use Only**

# Förster Resonance Energy Transfer inside Hyperbolic Metamaterials

*Diane J. Roth, Mazhar E. Nasir, Pavel Ginzburg, Pan Wang, Alix Le Marois, Klaus Suhling, David Richards and Anatoly V. Zayats*

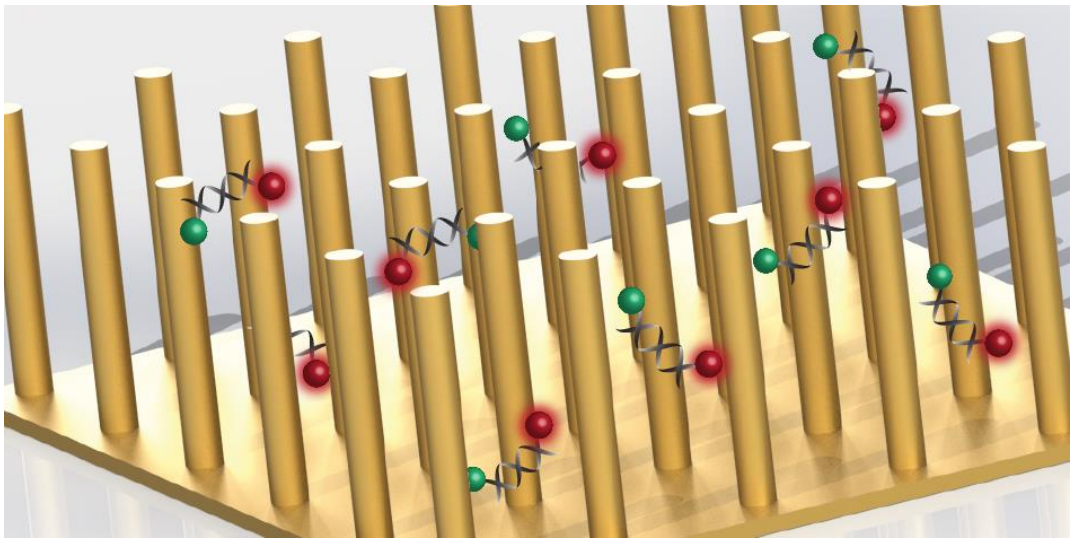

Double-stranded DNA donor-acceptor pairs embedded in a gold nanorod array were used to investigate FRET processes inside the hyperbolic metamaterial.